The synthesis and biological applications of photo-activated ruthenium anticancer drugs

Lameijer, L.N.

Chapter 1:

General introduction

1.1 Introduction: Transition metals in medicine

Since the discovery of arsenic based salvarasan (Figure 1.1a) as a first chemotherapeutic agent against syphilis, the field of bioinorganic (medicinal) chemistry has made a great leap forward. Imaging agents containing Gd^{III} ions have proven to be useful in MRI diagnostic studies due to their unique magnetic properties, resulting from their large number of unpaired electrons and long electron-spin relaxation times.[1] The complexes Dotarem® and Omniscan® have shown to be indispensable in modern tumor detection and imaging of blood vessels in the brain, spine or liver.[2] Furthermore, the application of metal complexes of the metastable isotope ^{99m}Tc have shown their value in radiotherapy for diagnostic imaging. Examples of such compounds are Cardiolite® and Ceretec®, which are clinically used for the evaluation of stroke and myocardial perfusion imaging, respectively.[1] However, one of the greatest accomplishments in the field of bioinorganic medicinal chemistry has been the discovery of cisplatin. Nowadays, this drug and its derivatives carboplatin and oxaliplatin (Figure 1.2) are the most widely used drugs against cancer.[1]

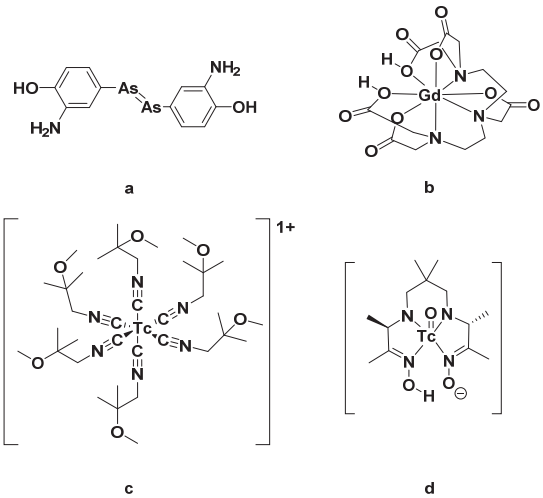

Figure 1.1. (a) Salvarasan , (b) Dotarem®, (c) Cardiolite® and (d) Ceretec®.

1.2 Cancer

Cancer is a group of diseases defined by unregulated cell growth and the invasion and migration of cells to neighboring tissue.[3] Cancer starts at a genomic level where deleterious mutations to DNA that are not repaired by DNA repair mechanisms such as nucleotide excision repair (NER), and that are passed on to daughter generations, can lead to the formation of oncogenes. These genes, which are involved in regulation of cell growth, cell differentiation or cell death can together with mutated tumor suppressor genes, lead to the formation of cancer.[3] With a mortality rate of 171 per 100.000 men and women per year (2008-2012) this disease is one of the leading causes of death in the United States.[4] Current treatments against cancer are roughly divided in four types:

surgery, radiotherapy, immunotherapy and chemotherapy.[5] In chemotherapy, platinum-based medicines are used in 50% of the cases.[6] The next section will focus on the discovery of cisplatin and the further study of transition metal based chemotherapeutics.

1.2.1 Pt-based anticancer drugs

Barnett Rosenberg observed that *E. Coli* bacteria showed unusual growth behavior when grown in an ammonium chloride buffer while a current was applied. It was found that this effect could be ascribed to the platinum hydrolysis byproducts formed by the 'inert' platina electrodes. Further investigations showed that the inhibition of cell division was caused by the most active species *cis*-$[PtCl_4(NH_3)_2]$ and *cis*-$[PtCl_2(NH_3)_2]$. These species were further considered for anticancer studies. After successful testing against a cancer cell line in mice and a further decade of clinical testing, cisplatin received FDA approval in 1978 and is now one of the most successful drugs used against cancer.[7]

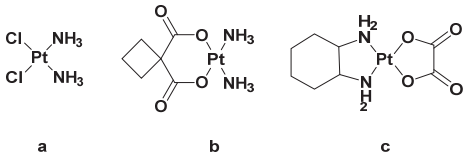

Figure 1.2. Chemical structures of (a) cisplatin, (b) carboplatin and (c) oxaliplatin.

The cytotoxic effect of the drug is attributed to the interaction of the aquated species *cis*-$[Pt(NH_3)_2(H_2O)_2]^{2+}$ with nuclear DNA resulting in a cascade of biological processes, leading to apoptosis of the cell.[8] After intravenous administration the drug enters the bloodstream and stays mostly intact due to the relatively high concentration of chloride anions in the blood plasma (100 mM), preventing hydrolysis of the complex. However, after diffusion of the complex through the cell membrane, or upon cellular uptake mediated by a copper transporter, the complex hydrolysis inside the cell due to the low concentration of chloride ions in the cytoplasm (~4 mM), forming a positively charged reactive species that cannot pass lipid bilayers.[8] This species either forms a monofunctional DNA adduct *via N*7 of guanine, or a bifunctional DNA adduct which cause a major distortion of the DNA, thereby preventing transcription. This DNA platination either triggers repair mechanisms such as nucleotide excision repair (NER) to repair DNA, which, when upregulated, leads to drug resistance, or to programmed cell death such as apoptosis and subsequent tumor elimination.[9] Some cancers are intrinsically resistant against cisplatin, while others develop this resistance after prolonged exposure. Such drug resistance has been also attributed to increased levels of the 'scavenger' tripeptide glutathione or metallothionein, which leads to a decreased intracellular accumulation of cisplatin and increased tolerance of the DNA adducts.[9] Although the side-effects of cisplatin and drug resistance can be circumvented using different analogues such as oxaliplatin and carboplatin, the overall disadvantages of these type of drugs have

stimulated the scientific community to investigate alternative compounds based on other transition metals.[10]

1.2.2 Ru-based anticancer drugs

Among the other transition metals, metal complexes of ruthenium have shown promising activity against cancer.[11] Ruthenium is located in group 8 of the periodic table and proved its potential value for use in anticancer drugs when Dwyer and coworkers found that tris(3,4,7,8-tetramethyl-1,10-phenanthroline)ruthenium(II) dichloride showed some inhibitory effects on the growth of Landschütz ascites tumor in mice.[12] For the past twenty years, complexes of this metal have demonstrated to have great potential both *in vitro* and *in vivo*.[13] Two of the most studied ruthenium drugs are NAMI-A ([H_2Im][trans-$RuCl_4$(DMSO)(Im)]) (Im = imidazole, DMSO = dimethylsulfoxide) and KP1019 (*trans*-[tetrachloridobis(1*H*-indazolium)ruthenate(III)). NAMI-A (Figure 1.3a) has low potency against primary tumors *in vitro*, but it has shown to be very effective against tumor metastasis *in vivo*.[14] KP1019 (Figure 1.3b) on the other hand, has shown great promise *in vitro* against several cancer cell lines[15] and entered Phase I clinical trials.[15] However, poor water-solubility of this compound halted further investigation. Currently the more water-soluble sodium derivative of KP1019, KP1339 (Figure 1.3c) is under investigation in a phase I clinical trial too.[16] Many other potent ruthenium-based anticancer drugs and their modes of action are described in the literature, but this is reviewed elsewhere.[17]

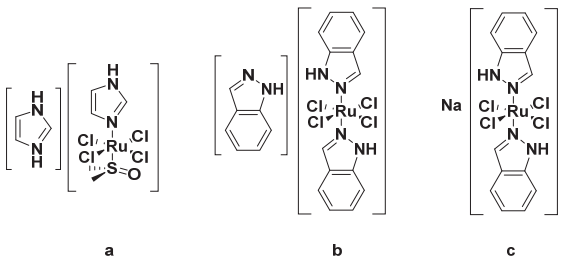

Figure 1.3. NAMI-A (a), KP-1019 (b) and KP-1339 (c).

1.3 Light and medicine

Next to their anticancer properties ruthenium(II) derivatives are excellent candidates for phototherapy. Their ability to absorb light in the visible region (400 – 700 nm) of the electromagnetic spectrum due to very strong metal-to-ligand charge transfer (MLCT) bands is often accompanied by photochemical processes such as photoreduction,[18] oxidation,[18] luminescence,[19] isomerization[20] or substitution.[21] The outcome of the competition between these different photochemical processes can be fine-tuned: by modulating the ligands bound to ruthenium, phosphorescence can be enhanced or diminished, as well as the generation of singlet oxygen ($^1O_2$). Exploiting the latter phenomenon to selectively damage cancer tissue is referred to as photodynamic therapy

(PDT) and allows spatial and temporal control over toxicity of the drug. It has been proposed for the treatment of easily accessible tumors (e.g. skin, neck, head and mouth) but also of more difficult tumors such as prostate, pancreatic and brain tumours using interstitial PDT (I-PDT).[22] Two types of PDT are generally distinguished, both of which are catalytic processes.[23] In PDT Type I the photosensitizer is excited by the absorption of a photon and after inter-system crossing, reacts from the generated triplet state with molecular dioxygen directly via an electron-transfer mechanism (Figure 1.4) to a superoxide. In PDT type II, the photosensitizer reaches an excited state, which is followed by inter-system-crossing to a triplet state from which the photosensitizer reacts with molecular dioxygen ($^3O_2$) via triplet-triplet annihilation (TTA). This leads to the generation of singlet dioxygen ($^1O_2$), which is highly reactive and can oxidize a whole range of substrates, including biomolecules such as lipids in the cell membrane, cofactors, or proteins. Such irreversible damage typically leads to cell death, tumor elimination and a response from the immune system.[24]

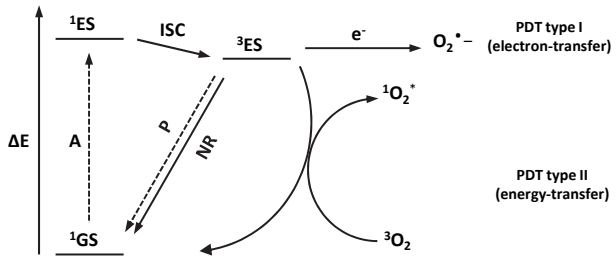

Figure 1.4. Jablonski diagram of photophysical pathways in photodynamic therapy type I and II with molecular oxygen. Dashed lines indicate processes involving photons. Abbreviations: GS (ground state), A (absorption), ES (excited state), ISC (inter-system crossing), P (phosphorescence), NR (non-radiative decay).

1.3.1 PDT with ruthenium(II) polypyridyl drugs

Ruthenium(II) photosensitizers have many advantages over classical PDT photosensitizers such as Foscan® and Photofrin®: they have increased water-solubility, long-lived triplet states, low toxicity in the dark and poor photobleaching.[24] The group of Gasser has demonstrated the merit of using ruthenium compound by combining targeted delivery and $^1O_2$ generation. Complexes based upon the $[Ru(bpy)_2(dppz)]^{2+}$ (bpy = 2,2'-bipyridine, dppz = dipyrido[3,2-*a*:2',3'-*c*]phenazine) scaffold were designed with minor modifications on the planar dipyridophenazine ring. It was found that this complex (Figure 1.5a) had a remarkable activity against HeLa cancer cells when an amine was introduced. The cytotoxicity before light-activation, which is typically expressed as the effective concentration EC_{50} (the concentration at which 50% of the cells are dead compared to untreated control), was much lower than the cytoxicity after light irradiation. Photoindices (PI), which are defined as the ratio $EC_{50dark}/EC_{50light}$, can reach up to 150. Due to its luminescent properties visualization and localization of this compound in HeLa cell was

possible; it was found to accumulate in the nucleus. This was further confirmed by fractionation experiments and high-resolution continuum source atomic absorption spectrometry (HR-CS AAS).[25] Using a different approach, the group of Turro demonstrated that $[Ru(bpy)(dppn)(CH_3CN)_2]^{2+}$ (Figure 1.5b) was able to both photosubstitute one monodentate ligand and generate $^1O_2$, leading to submicromolar photocytotoxicity in HeLa cells.[26] However, the most promising candidate among the ruthenium(II) polypyridyl drugs was recently reported by the group of McFarland: The compound, $[Ru(dmb)_2(IP\text{-}TT)]^{2+}$ (dmb = 4,4'-dimethyl-2,2'-bipyridine, IP-TT = 2-(2',2'':5'',2'''-terthiophene)-imidazo[4,5-f][1,10]phenanthroline) also referred to as TLD1433 (Figure 1.5c), demonstrated to have great potential in both colon and glioma cancer cells, reaching PI values over 10000.[27] This drug is currently under investigation in Phase I clinical trials (NCT03053635).

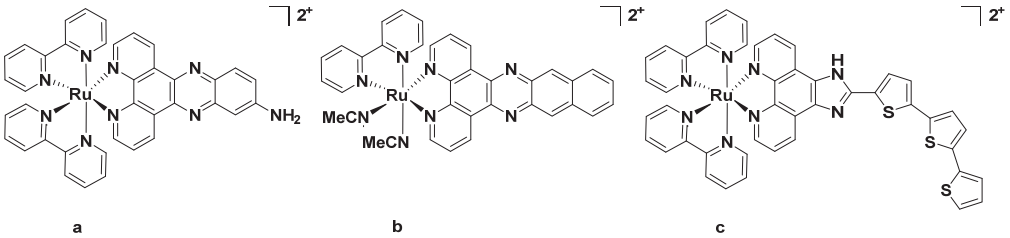

Figure 1.5. Representative examples of ruthenium(II) polypyridyl PDT drugs from the groups of (a) Gasser,[28] (b) Turro,[29] and (c) McFarland.[24]

1.3.2 Tumor hypoxia and PDT

Due to rapid cell proliferation and structural and functional abnormalities in tumor blood vessels, certain regions in solid tumors are poorly oxygenated.[30] This phenomenon was first observed by Grey et. al.[31] and has a serious impact on the effectiveness of conventional treatments such as radiation therapy.[32] For PDT type II a similar problem arises since the therapy is dioxygen-dependent (unlike PDT type I, which occurs via electron-transfer). In addition, PDT often results in additional hypoxia by consumption of the oxygen on the tumor site while simultaneously inducing damage to the tumor vasculature, preventing the consumed dioxygen to be renewed.[22a, 33]

1.3.3 Photo-Chemotherapy (PCT) or Photo-Activated Chemotherapy (PACT)

The oxygen-dependence of PDT provides an incentive to develop anticancer agents that operate via a different, dioxygen-independent mode of action.[11] Instead of generating $^1O_2$, these light-sensitive prodrugs become cytotoxic after photoisomerization,[34] photoreduction,[35] photocleavage,[36] or photosubstitution.[37] The last two mechanisms are often referred to as photo-uncaging and 'Photo-Activated ChemoTherapy' (PACT) when they are used in combination with cytotoxic anticancer drugs. In PACT the prodrug is not active (caged) in the dark, whereas light-activation leads to bond cleavage (uncaging) of the prodrug, releasing both the (cytoxotoxic) carrier and/or a drug payload.[38]

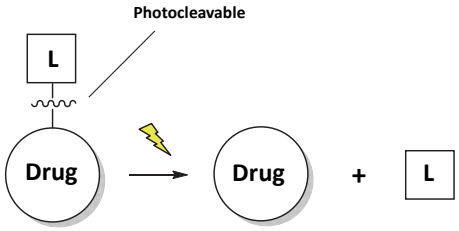

Figure 1.6. Principle of PACT.[36, 38] Upon irradiation bond cleavage leads to release of a metal-based or ligand-based drug.

Several organic and inorganic systems for photo-release of cytotoxic drugs have been used by the scientific community. These prodrugs either work independently or in combination with a drug delivery system such as nanoparticles. In 2010, Lin et. al demonstrated an amino-coumarin system that, attached to a mesoporous nanoparticle, released chloroambucil using visible light (420 nm) and induced cytotoxicity in HeLa cells.[39] More recently, Nani et. al. have further demonstrated that a cyanine-based photocaging agent can be combined with an antibody-drug conjugate, allowing release with near-infrared light (NIR) of a microtubule polymerization inhibitor combretastatin A4. Cytotoxicity was induced both *in vitro* and *in vivo*.[40]

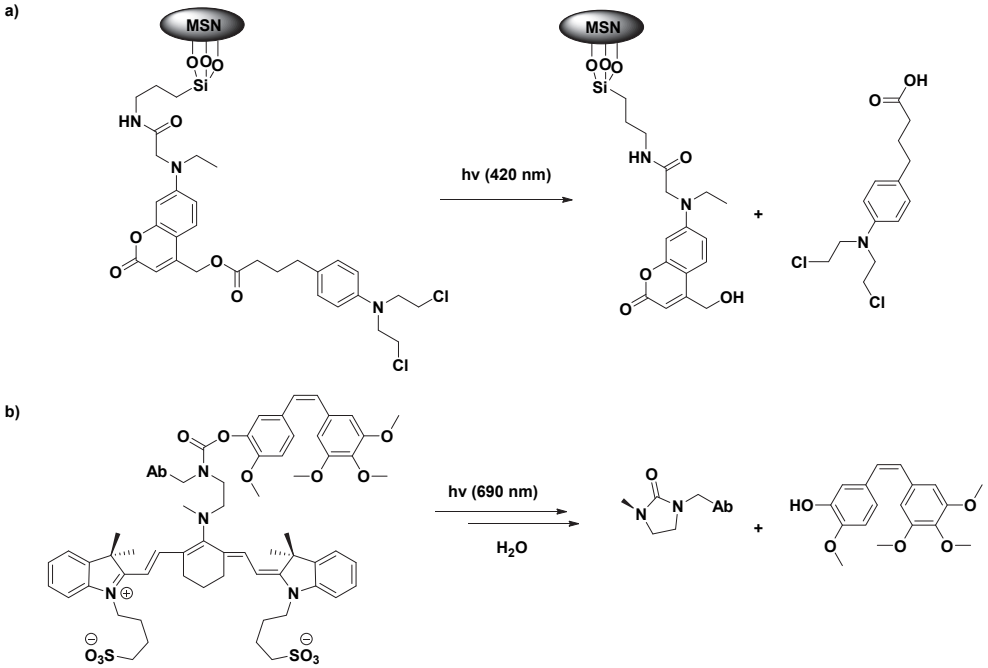

Figure 1.7. a). Mesoporous nanoparticles (MSN) covalently attached to amino coumarin based photocaged chloroambucil. b). Antibody-targeted cyanine-based photocaging system, releasing combrestatin A4 after irradiation with NIR light. Photo-oxidation, hydrolysis and cyclization steps have been omitted for clarity.

In the field of bioinorganic chemistry, examples of photocaging systems have been reported by the group of Gasser who have demonstrated the targeted delivery of rhenium-bombesin conjugates caged with *o*-nitrophenyl-based photo-linkers. Uncaging with low doses of UV-light led to the release of a tricarbonyl *N,N*-bis(quinolinoyl) rhenium (I) complex, achieving a ten-fold higher cytotoxicity towards HeLa cells than without irradiation.[36] A ruthenium-based photocaging system utilizing nanoparticles has been reported by Frasconi et. al in 2013. Paclitaxel loaded mesoporous nanoparticles were 'capped' with $[Ru(tpy)(dppz)(L)]^{2+}$ (tpy = 2,2':6',2''-terpyridine) complexes, releasing the anticancer drug after photo-activation with visible light (465 nm), which led to a marked decrease in cell viability in MDA-MB-231 and MDA-MB-248 cells.[41] The research described in this thesis will focus on the latter types of systems, where ruthenium(II) polypyridyl drugs are used either as a PACT drug or PACT carrier using photosubstitution to release a cytotoxic drug or to induce cytotoxicity by themselves.

1.3.4 Ruthenium-based PACT

The mechanism of photosubstitution of ruthenium(II) (polypyridyl) compounds is generally thought to occur as follows: after absorption of a photon the metal-to-ligand charge-transfer state (^{1}MLCT) is populated via photon absorption by the ground state (^{1}GS), which is immediately followed by inter-system-crossing to the ^{3}MLCT state. This state can decay to the ground state *via* radiative or non-radiative processes, or populate the triplet metal-centered state (^{3}MC) via thermal internal conversion (IC). Due to the antibonding character of the orbitals (dσ) in this state, population of this state leads to elongation of a metal-ligand bond and ligand dissociation.[29, 42] Since ruthenium(II) is a d^6 metal with an octahedral configuration, ligands such as tpy can reduce the coordination angles, leading to distorted pseudo-octahedral geometries in which the nitrogen lone pairs of the polypyridyl ligands have less overlap with the orbitals of the ruthenium center.[43] This leads to smaller ligand field splitting compared to, for example, complexes such as $[Ru(bpy)_3]^{2+}$. This octahedral distortion leads to an ^{3}MC excited state that is lower in energy, and thus more easily thermally populated from the ^{3}MCLT.

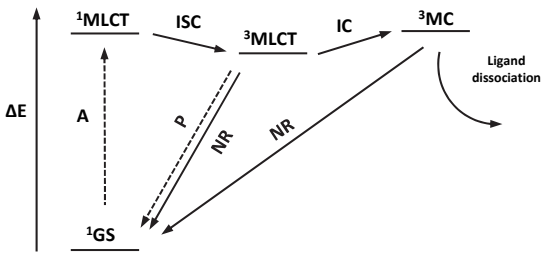

Figure 1.8. Jablonski diagram of proposed physical pathways of photosubstitution reactions in Ru(II) polypyridyl complexes. Dashed arrows represent pathways involving a photon. Abbrevations: GS (ground state), A (absorption), ISC (inter-system crossing), P (phosphorescence), NR (non-radiative decay), IC (internal conversion), MC (metal centered).

One of the first groups to find an application of these ruthenium complexes in chemical biology and phototherapy was that of Etchenique, who delivered a proof-of-concept that the biologically active ligand 4-aminopyridine (4AP) could be released from the complex $[Ru(bpy)_2(4AP)_2]Cl_2$.[44] After irradiation with white light (>500 nm) in water, this complex selectively photosubstitutes one of the 4AP monodentate ligands for water, releasing free 4AP which induces an action potential in leech neurons.[44] A similar demonstration leading to phototoxicity in cancer cells was first provided by the group of Turro, who demonstrated that photorelease in HeLa cells of 5-cyanouracil (5CNU), a known anticancer drug, by irradiation with white light (>400 nm) of $[Ru(tpy)(5CNU)_3]^{2+}$, leads to cell death.[45] Turro also demonstrated that the released ruthenium species $[Ru(tpy)(5CNU)(H_2O)_2]^{2+}$ is able to bind to DNA, implying that this species may contribute to the observed cellular toxicity.[45] A more recent example from 2012 by Howerton et. al. has demonstrated that the strained complex $[Ru(bpy)_2(dmbpy)]^{2+}$ (bpy = bipyridine, dmbpy = 6,6'-dimethyl-2,2'-dipyridyl) ejects a dmbpy ligand upon white light irradiation (>450 nm), generating the ruthenium species $[Ru(bpy)(H_2O)_2]^{2+}$ which was also found to be able to bind to DNA. The observed cytotoxicity in A549 tumor spheroids was attributed to the generation of this species.

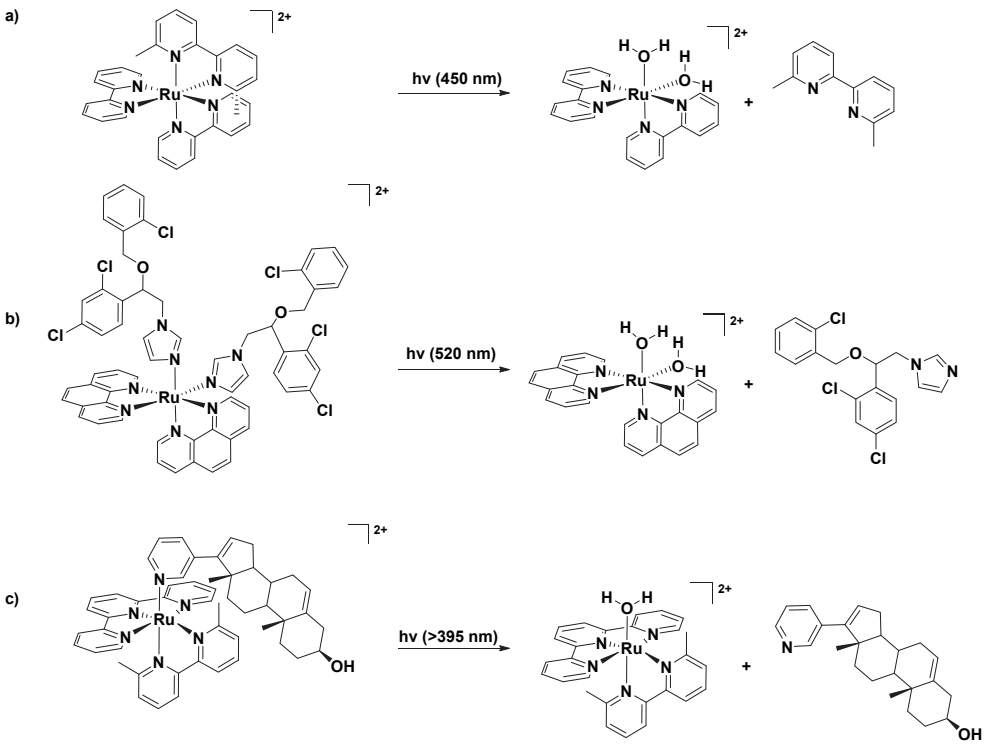

Figure 1.9. Representative ruthenium-based PACT drugs by the group of (a) Bonnet/Glazer,[46] (b) Renfrew[47] and (c) Kodanko.[48]

This claim, however, was recently refuted by Cuello-Garibo and coworkers followed by Azar et. al.[46a, 49] who independently demonstrated that the expulsed ligand (dmbpy) was cytotoxic. Nevertheless, Howerton's work demonstrated that these complexes can be used to kill cancer cells using visible light *via* a dioxygen-independent mechanism, i.e., the release of the cytotoxic ligand dmbpy. More examples of ruthenium-based anticancer PACT drugs have been described by the group of Kodanko,[48] Renfrew[47] and Bonnet[50] with some noteworthy examples of PACT drugs shown in Figure 1.9.

1.4 Selective treatment of cancer

Conventional anticancer drugs, such as cisplatin, generally affect both malignant and healthy cells, thereby reducing the maximum dosage which can be administered to a patient.[51] One approach to improve selectivity and reduce the side effects for patients is to conjugate the anticancer drugs to a 'homing beacon' that specifically targets receptors that are overexpressed in cancer cells. This 'Trojan horse' approach has been successfully demonstrated by the clinically approved brentuximab vedotin in Hodgkin lymphoma and Trastuzumab emtansine in HER2-positive metastatic breast cancer. Other examples encompass folate receptor targeted therapy,[52] a receptor that is overexpressed in ovarian cancers, the use of liposomes, such as demonstrated for lipoplatin,[53] and the focus of the next section, glucose transporter (GLUT) targeted therapy.[54]

1.4.1 Targeting GLUT

Tumorigenesis is hallmarked by some crucial alterations to cellular metabolism. One of the best characterized metabolic phenotypes in cancer is the increase of aerobic glycolysis for the generation of adenosine triphosphate (ATP), also known as the "Warburg effect".[55] Even in the presence of normal concentrations of dioxygen in cancer cells, D-glucose is converted to lactic acid rather than using oxidative phosphorylation for the generation of ATP. It has been suggested that this phenomenon occurs for a powerful growth advantage and is necessary for the evolution of invasive human cancers.[56] One of the consequences of this phenomenon is the overexpression of glucose transporters (GLUTs)[57] in proliferating tumor cells: a family of thirteen different proteins (GLUT 1 – 12 and HMIT) responsible for the energy-independent uptake of monosaccharides and polyols in mammalian cells.[58] GLUT1 and GLUT3 are predominantly overexpressed in most cancers, making it an important cancer hallmark and potential target in targeted chemotherapy.[54, 56]

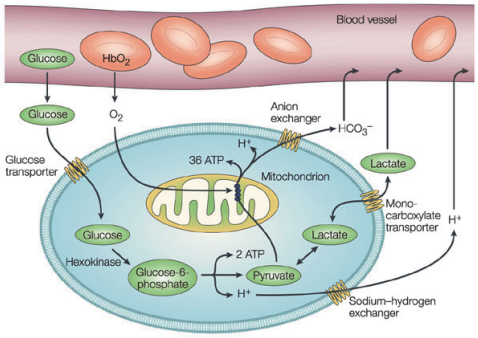

Figure 1.10. Glucose metabolism in healthy mammalian cells. Figure taken from Gatenby et. al.[56]

The field of diagnosis imaging has exploited the Warburg effect for positron emission tomography (PET) using ^{18}fluorodeoxyglucose (^{18}FDG) (Figure 1.11a). This compound is a radioactive labeled derivative of D-glucose, which is taken up *via* GLUT1 and subsequently trapped by hexokinase mediated phosphorylation allowing for tumor visualization.[56] This hallmark has further been explored as a potential target in the field of medicinal chemistry by Wiessler and coworkers.[59] Due to the heavy adverse side-effects of the widely used ifosfamide alkylating agent as antitumor drug, an alternative was found in its D-glucose derivative glufosfamide (Figure 1.11b). Compared to its aglycon, this compound was found to be less cytotoxic and could be administered in higher doses without affecting healthy cells.[59] Other examples of glycoconjugated anticancer drugs have been reported by Mandai and Mikuni and coworkers in 2008.[60] They revealed that the α-galactosyl conjugate of docetaxel (Figure 1.11c) widely used against breast, ovarian, prostate and non-small lung cancer, showed similar cytotoxic activity against P388 Murine Leukemia Cells compared to its aglycon. It was envisioned that this derivative is more water-soluble and therefore co-administration of solubilizing agents is not necessary.[60]

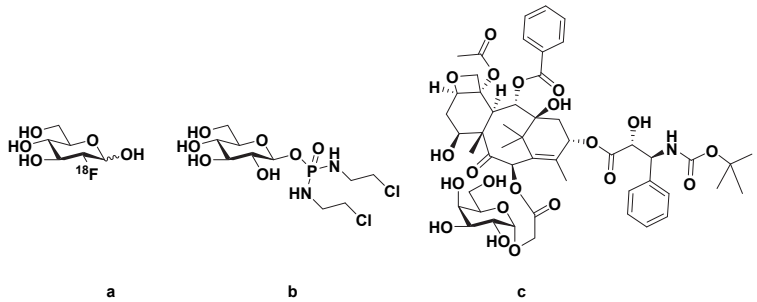

Figure 1.11. Overview of GLUT transported D-glucose and D-galactose conjugates. a). ^{18}FDG b). Glufosfamide; c). 1-α-D-galactose conjugated docetaxel.

1.4.2 Substrate specificity

The selective targeting of cancer cells using glycoconjugates calls for a study of substrate specificity. As of date, both the structures of human GLUT1 and GLUT3 have been

elucidated.[61] Whereas GLUT1 was co-crystallized in the presence of *n*-nonyl-β-D-glucopyranoside, GLUT3 tolerated both the α and β-anomer of D-glucose[61] suggesting that 1-*O*-β-modifications, such as for glufosfamide (Figure 1.11b), are generally allowed. Both 2-(N-(7-nitrobenz-2-oxa-1,3-diazol-4-yl)amino)-2-deoxyglucose (NBDG) and FDG are modified on the 2-position of D-glucose, indicating that modification of this position is tolerated. Reports of glycoconjugates with modifications on the *O*-3, *O*-4 and *O*-6 position of D-glucose and their uptake by GLUT1 are abundant in literature, with the overall conclusion that, unless very bulky groups are installed, most positional modifications are tolerated.[54] However a recent example by Park et. al. has shown that the overall charge of β-glycosidic cyanine based bioprobes might influence the uptake by GLUT1.[62]

This raises the question whether this strategy can also be applied for metal complexes for radiotherapy or as potential theranostics. In the field of bioinorganic chemistry the group of Schubiger pioneered this strategy in 2001 with the synthesis of rhenium and ^{99m}Tc glycoconjugates.[63] This work was followed with a whole mechanistic study and uptake study reported in 2005,[64] which demonstrated that *O*-1, *O*-2 (Figure 1.12a), *O*-3 and *O*-6 glycoconjugates of ^{99m}Tc drugs were not taken up via GLUT1 in HT29 cells. No differences in uptake were observed in the presence of the GLUT1 inhibitor cytochalasin B and D-glucose.[64] This is in great contrast to the recent findings of Patra et. al.[65] who have demonstrated that *O*-2 glycoconjugates (Figure 1.12b) of a platinum-based drug (malonatoplatin) were taken up in an increased manner in A549 cells, compared to other positional isomers. The uptake in healthy RWPE2 cells, however, was similar among conjugates, implying that the higher expression of GLUT in A549 cancer cells has a strong effect on the uptake. This was further supported by using a DU145-GLUT1-knock-down cell-line that showed that the glycoconjugate was less toxic when GLUT-1 was not present. A recent example by Florindo et. al. has suggested that uptake of cyclopentadienyl-ruthenium(II) glycoconjugates is possible. The cell cytotoxicity induced by their glycoconjugate (Figure 1.12c) could be reduced in the presence of D-glucose.[66] However, there is currently no general consensus as to which modifications of D-glucose are allowed in order to allow transport of antitumor drugs via GLUT1 or GLUT3 for ruthenium(II) drugs.

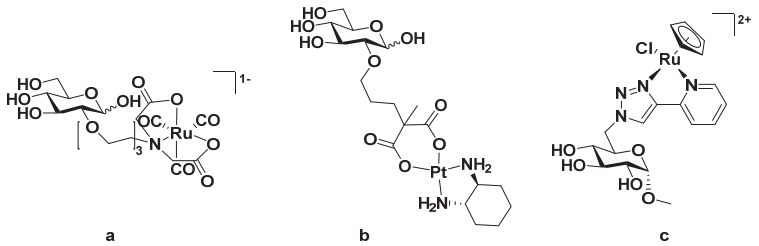

Figure 1.12. Representative glycoconjugates for GLUT targeting from the group of (a) Schubiger,[64] (b) Lippard[65b] and Fernandes.[66]

1.5 Thesis goal and outline

The aim of the work described in this thesis was to investigate whether complexes based upon the $[Ru(tpy)(N\text{-}N)(L)]^{n+}$ scaffold can be used either: (i) as a PACT prodrug where a toxic mono-aquated ruthenium complex is caged by a non-toxic ligand and liberated upon light irradiation; or (ii) as a PACT carrier for photocaging, where a thioether, nitrile or pyridine-based organic drug is caged by a non-toxic ruthenium fragment, and released upon light irradiation; (iii) or as a PDT prodrug, where reactive oxygen species (ROS) are generated upon blue, green or red light irradiation of the metal complex.

In Chapter **2** new synthetic routes are described towards methylthioether-functionalized positional isomers of D-glucose and their ruthenium polypyridyl conjugates. Due to the coordinating properties of the sulfur donor atoms in these ligands different protecting and deprotecting group strategies had to be employed compared to that for example of Lippard et. al.,[65b] since the common benzyl and benzylidene protecting group cannot be efficiently removed in the presence of a thioether using palladium on carbon or a Birch reduction. The proposed routes for the most challenging 2-*O* and 4-*O* functionalized isomers are improvements over current strategies as they can potentially be used for ligands bearing sulfur (or nitrogen) donor atoms.

In Chapter **3** a new strategy is presented to analyze the effects of glycoconjugation on ruthenium anticancer prodrugs of the type $[Ru(tpy)(dppn)(L)]^{2+}$. Two enantiomers of glycoconjugated prodrugs are presented which are both activated with blue light. Light irradiation makes them strongly cytotoxic, which is demonstrated to be a consequence of their localization in the mitochondria where they efficiently generate ROS. Interestingly, both enantiomers of the drugs showed similar uptake, which rules out GLUT-mediated transport, whereas the different dark cytotoxicity found for both enantiomers is most likely attributed to a post-uptake process such as hydrolysis by a β-glucosidase.

In Chapter **4** the influence of the bidentate ligand in sixteen complexes based upon the $[Ru(tpy)(N\text{-}N)(L)]^{2+}$ scaffold is described in relation to their photoreactivity, phosphorescence, singlet oxygen generation, and photosubstitution quantum yield. By comparing the (photo)cytotoxicity, solubility and uptake of these complexes in two different cancer cell lines (A549 and MCF-7), insight is provided on the potential of these compounds as light-activated prodrugs. Whereas most of these complexes are not (photo)cytotoxic and are therefore excellent candidates as PACT carriers, three complexes were found to be cytotoxic after blue light irradiation, and thus represent interesting PACT drugs. Depending on the treatment protocol the compounds $[Ru(tpy)(dppz)(L)]^{2+}$ were found to act as a potential PACT drug, while $[Ru(tpy)(dppn)(L)]^{2+}$ complexes were found to act as very efficient PDT sensitizers even when using a strict treatment protocol.

Chapter **5** describes the synthesis of a series of chiral cyclometalated ruthenium complexes based upon the $[Ru(phpy)(N\text{-}N)(dmso\text{-}kS)]^{2+}$ scaffold, where Hphpy is 6'-phenyl-2,2'-bipyridine. Cyclometalation appears to reduce the charge and polarity of terpyridine analogues while their absorption is shifted towards the red region of the spectrum. Three of these complexes with N-N = bpy, phen, and dpq, are much less photoreactive than the terpyridine analogues described in Chapter **4**, while the more conjugated dppz and dppn complexes are photochemically completely inactive. We demonstrate that these complexes are chiral by synthesizing and separating two diastereoisomers bound to a chiral, enantiomerically pure sulfoxide monodentate ligand. We finally show their potential as (green) light-activated anticancer drugs against A549 and MCF-7 cancer cells.

In Chapter **6** we demonstrate that both the $[Ru(tpy)(dmbpy)(L)]^{2+}$ and $[Ru(tpy)(biq)(L)]^{2+}$ scaffold can be used to cage L = STF-31, a pyridine-containing cytotoxic inhibitor of nicotinamide phosphoribosyltransferase (NAMPT). We show that both scaffolds can be uncaged using deeper tissue-penetrating red light, but that only $[Ru(tpy)(biq)(L)]^{2+}$ is thermally stable enough to be used *in vitro* as a prodrug. By studying photoactivation under hypoxia (1% O_2), we demonstrate for the first time that PACT works independently of the dioxygen concentration in cells, whereas traditional dioxygen-dependent PDT would not work under the same conditions.

Finally, a summary of the findings in this thesis are presented in Chapter **7,** followed by an outlook for ruthenium-based photoactivated prodrugs.

References

[1] Z. J. Guo, P. J. Sadler, *Angew Chem Int Ed* **1999**, *38*, 1513-1531.

[2] P. Caravan, J. J. Ellison, T. J. McMurry, R. B. Lauffer, *Chem Rev* **1999**, *99*, 2293-2352.

[3] L. Pecorino, *Molecular biology of cancer: mechanisms, targets, and therapeutics*, Oxford university press, **2012**.

[4] R. L. Siegel, K. D. Miller, A. Jemal, *CA Cancer J Clin* **2016**, *66*, 7-30.

[5] K. D. Miller, R. L. Siegel, C. C. Lin, A. B. Mariotto, J. L. Kramer, J. H. Rowland, K. D. Stein, R. Alteri, A. Jemal, *CA Cancer J Clin* **2016**, *66*, 271-289.

[6] S. Dhar, S. J. Lippard, *P Natl Acad Sci USA* **2009**, *106*, 22199-22204.

[7] a). S. M. Cohen, S. J. Lippard, *Prog Nucleic Acid Res Mol Biol* **2001**, *67*, 93-130; b). R. A. Alderden, M. D. Hall, T. W. Hambley, *J Chem Educ* **2006**, *83*, 728-734.

[8] S. Dasari, P. B. Tchounwou, *Eur J Pharmacol* **2014**, *740*, 364-378.

[9] L. R. Kelland, S. Y. Sharp, C. F. O'Neill, F. I. Raynaud, P. J. Beale, I. R. Judson, *J Inorg Biochem* **1999**, *77*, 111-115.

[10] P. C. Bruijnincx, P. J. Sadler, *Curr Opin Chem Biol* **2008**, *12*, 197-206.

[11] P. C. Bruijnincx, P. J. Sadler, *Adv Inorg Chem* **2009**, *61*, 1-62.

[12] F. P. Dwyer, E. Mayhew, E. M. F. Roe, A. Shulman, *Brit J Cancer* **1965**, *19*, 195-199.

[13] A. Bergamo, C. Gaiddon, J. H. Schellens, J. H. Beijnen, G. Sava, *J Inorg Biochem* **2012**, *106*, 90-99.

[14] A. Bergamo, S. Zorzet, B. Gava, A. Sorc, E. Alessio, E. Iengo, G. Sava, *Anticancer Drugs* **2000**, *11*, 665-672.

[15] C. G. Hartinger, S. Zorbas-Seifried, M. A. Jakupec, B. Kynast, H. Zorbas, B. K. Keppler, *J Inorg Biochem* **2006**, *100*, 891-904.

[16] A. K. Bytzek, G. Koellensperger, B. K. Keppler, G. H. C, *J Inorg Biochem* **2016**, *160*, 250-255.

[17] J. Liu, L. N. Ji, W. J. Mei, *Prog Chem* **2004**, *16*, 969-974.

[18] C. K. Prier, D. A. Rankic, D. W. MacMillan, *Chem Rev* **2013**, *113*, 5322-5363.

[19] K. Nakamaru, *Bull Chem Soc Jpn* **1982**, *55*, 2697-2705.

[20] H. Yamazaki, T. Hakamata, M. Komi, M. Yagi, *J Am Chem Soc* **2011**, *133*, 8846-8849.

[21] R. E. Goldbach, I. Rodriguez-Garcia, J. H. van Lenthe, M. A. Siegler, S. Bonnet, *Chem Eur J* **2011**, *17*, 9924-9929.

[22] a). D. E. Dolmans, D. Fukumura, R. K. Jain, *Nat Rev Cancer* **2003**, *3*, 380-387; b). J. F. Lovell, T. W. Liu, J. Chen, G. Zheng, *Chem Rev* **2010**, *110*, 2839-2857; c). G. Shafirstein, D. Bellnier, E. Oakley, S. Hamilton, M. Potasek, K. Beeson, E. Parilov, *Cancers* **2017**, *9*.

[23] A. P. Castano, T. N. Demidova, M. R. Hamblin, *Photodiagnosis Photodyn Ther* **2004**, *1*, 279-293.

[24] G. Shi, S. Monro, R. Hennigar, J. Colpitts, J. Fong, K. Kasimova, H. M. Yin, R. DeCoste, C. Spencer, L. Chamberlain, A. Mandel, L. Lilge, S. A. McFarland, *Coord Chem Rev* **2015**, *282*, 127-138.

[25] C. Mari, V. Pierroz, R. Rubbiani, M. Patra, J. Hess, B. Spingler, L. Oehninger, J. Schur, I. Ott, L. Salassa, S. Ferrari, G. Gasser, *Chem Eur J* **2014**, *20*, 14421-14436.

[26] B. A. Albani, B. Pena, N. A. Leed, N. A. de Paula, C. Pavani, M. S. Baptista, K. R. Dunbar, C. Turro, *J Am Chem Soc* **2014**, *136*, 17095-17101.

[27] J. Fong, K. Kasimova, Y. Arenas, P. Kaspler, S. Lazic, A. Mandel, L. Lilge, *Photobiol Sci* **2015**, *14*, 2014-2023.

[28] C. Mari, V. Pierroz, S. Ferrari, G. Gasser, *Chem Sci* **2015**, *6*, 2660-2686.

[29] J. D. Knoll, B. A. Albani, C. Turro, *Acc Chem Res* **2015**, *48*, 2280-2287.

[30] D. M. Gilkes, G. L. Semenza, D. Wirtz, *Nat Rev Cancer* **2014**, *14*, 430-439.

[31] R. H. Thomlinson, L. H. Gray, *Brit J Cancer* **1955**, *9*, 539-549.

[32] L. H. Gray, A. D. Conger, M. Ebert, S. Hornsey, O. C. Scott, *Br J Radiol* **1953**, *26*, 638-648.

[33] B. W. Henderson, V. H. Fingar, *Cancer Res* **1987**, *47*, 3110-3114.

[34] M. M. Lerch, M. J. Hansen, G. M. van Dam, W. Szymanski, B. L. Feringa, *Angew Chem Int Ed* **2016**, *55*, 10978-10999.

[35] N. J. Farrer, J. A. Woods, V. P. Munk, F. S. Mackay, P. J. Sadler, *Chem Res Toxicol* **2010**, *23*, 413-421.

[36] A. Leonidova, V. Pierroz, R. Rubbiani, Y. J. Lan, A. G. Schmitz, A. Kaech, R. K. O. Sigel, S. Ferrari, G. Gasser, *Chem Sci* **2014**, *5*, 4044-4056.

[37] N. J. Farrer, J. A. Woods, L. Salassa, Y. Zhao, K. S. Robinson, G. Clarkson, F. S. Mackay, P. J. Sadler, *Angew Chem Int Ed* **2010**, *49*, 8905-8908.

[38] J. Olejniczak, C. J. Carling, A. Almutairi, *J Control Release* **2015**, *219*, 18-30.

[39] Q. Lin, Q. Huang, C. Li, C. Bao, Z. Liu, F. Li, L. Zhu, *J Am Chem Soc* **2010**, *132*, 10645-10647.

[40] R. R. Nani, A. P. Gorka, T. Nagaya, H. Kobayashi, M. J. Schnermann, *Angew Chem Int Ed* **2015**, *54*, 13635-13638.

[41] M. Frasconi, Z. Liu, J. Lei, Y. Wu, E. Strekalova, D. Malin, M. W. Ambrogio, X. Chen, Y. Y. Botros, V. L. Cryns, J.-P. Sauvage, J. F. Stoddart, *J Am Chem Soc* **2013**, *135*, 11603-11613.

[42] a). J. D. Knoll, B. A. Albani, C. B. Durr, C. Turro, *J Phys Chem A* **2014**, *118*, 10603-10610; b). P. C. Ford, *Chem Sci* **2016**, *7*, 2964-2986.

[43] A. J. Gottle, F. Alary, M. Boggio-Pasqua, I. M. Dixon, J. L. Heully, A. Bahreman, S. H. Askes, S. Bonnet, *Inorg Chem* **2016**, *55*, 4448-4456.

[44] L. Zayat, C. Calero, P. Albores, L. Baraldo, R. Etchenique, *J Am Chem Soc* **2003**, *125*, 882-883.

[45] M. A. Sgambellone, A. David, R. N. Garner, K. R. Dunbar, C. Turro, *J Am Chem Soc* **2013**, *135*, 11274-11282.

[46] a). J. A. Cuello-Garibo, M. S. Meijer, S. Bonnet, *Chem Commun* **2017**, *53*, 6768-6771; b). B. S. Howerton, D. K. Heidary, E. C. Glazer, *J Am Chem Soc* **2012**, *134*, 8324-8327.

[47] N. Karaoun, A. K. Renfrew, *Chem Commun* **2015**, *51*, 14038-14041.

[48] A. Li, R. Yadav, J. K. White, M. K. Herroon, B. P. Callahan, I. Podgorski, C. Turro, E. E. Scott, J. J. Kodanko, *Chem Commun* **2017**, *53*, 3673-3676.

[49] D. F. Azar, H. Audi, S. Farhat, M. El-Sibai, R. J. Abi-Habib, R. S. Khnayzer, *Dalton Trans* **2017**, *46*, 11529-11532.

[50] V. H. S. van Rixel, B. Siewert, S. L. Hopkins, S. H. C. Askes, A. Busemann, M. A. Siegler, S. Bonnet, *Chem Sci* **2016**, *7*, 4922-4929.

[51] K. Cho, X. Wang, S. Nie, Z. G. Chen, D. M. Shin, *Clin Cancer Res* **2008**, *14*, 1310-1316.

[52] R. T. Morris, R. N. Joyrich, R. W. Naumann, N. P. Shah, A. H. Maurer, H. W. Strauss, J. M. Uszler, J. T. Symanowski, P. R. Ellis, W. A. Harb, *Ann Oncol* **2014**, *25*, 852-858.

[53] T. Boulikas, *Expert Opin Investig Drugs* **2009**, *18*, 1197-1218.

[54] E. C. Calvaresi, P. J. Hergenrother, *Chem Sci* **2013**, *4*, 2319-2333.

[55] O. Warburg, F. Wind, E. Negelein, *Klin Wochenschr* **1926**, *5*, 829-832.

[56] R. A. Gatenby, R. J. Gillies, *Nat Rev Cancer* **2004**, *4*, 891-899.

[57] M. L. Macheda, S. Rogers, J. D. Best, *J Cell Physiol* **2005**, *202*, 654-662.

[58] M. Mueckler, B. Thorens, *Mol Aspects Med* **2013**, *34*, 121-138.

[59] J. Pohl, B. Bertram, P. Hilgard, M. R. Nowrousian, J. Stuben, M. Wiessler, *Cancer Chemother Pharmacol* **1995**, *35*, 364-370.

[60] K. Mikuni, K. Nakanishi, K. Hara, K. Hara, W. Iwatani, T. Amano, K. Nakamura, Y. Tsuchiya, H. Okumoto, T. Mandai, *Biol Pharm Bull* **2008**, *31*, 1155-1158.

[61] a). D. Deng, C. Xu, P. Sun, J. Wu, C. Yan, M. Hu, N. Yan, *Nature* **2014**, *510*, 121-125; b). D. Deng, P. Sun, C. Yan, M. Ke, X. Jiang, L. Xiong, W. Ren, K. Hirata, M. Yamamoto, S. Fan, N. Yan, *Nature* **2015**, *526*, 391-396.

[62] J. Park, J. I. Um, A. Jo, J. Lee, D. W. Jung, D. R. Williams, S. B. Park, *Chem Commun* **2014**, *50*, 9251-9254.

[63] J. Petrig, R. Schibli, C. Dumas, R. Alberto, P. A. Schubiger, *Chem Eur J* **2001**, *7*, 1868-1873.

[64] R. Schibli, C. Dumas, J. Petrig, L. Spadola, L. Scapozza, E. Garcia-Garayoa, P. A. Schubiger, *Bioconjugate Chem* **2005**, *16*, 105-112.

[65] a). M. Patra, T. C. Johnstone, K. Suntharalingam, S. J. Lippard, *Angew Chem Int Ed* **2016**, *55*, 2550-2554; b). M. Patra, S. G. Awuah, S. J. Lippard, *J Am Chem Soc* **2016**, *138*, 12541-12551.

[66] P. R. Florindo, D. M. Pereira, P. M. Borralho, P. J. Costa, M. F. Piedade, C. M. Rodrigues, A. C. Fernandes, *Dalton Trans* **2016**, *45*, 11926-11930.